GEOPHYSICS, VOL. 75, NO. 5 (SEPTEMBER-OCTOBER 2010); P. D37–D45, 8 FIGS.
10.1190/1.3481702

Localized anisotropic tomography with well information in VTI media

Andrey Bakulin[1], Marta Woodward[2], Dave Nichols[2], Konstantin Osypov[2], and Olga Zdraveva[2]

ABSTRACT

We develop a concept of localized seismic grid tomography constrained by well information and apply it to building vertically transversely isotropic (VTI) velocity models in depth. The goal is to use a highly automated migration velocity analysis to build anisotropic models that combine optimal image focusing with accurate depth positioning in one step. We localize tomography to a limited volume around the well and jointly invert the surface seismic and well data. Well information is propagated into the local volume by using the method of preconditioning, whereby model updates are shaped to follow geologic layers with spatial smoothing constraints. We analyze our concept with a synthetic data example of anisotropic tomography applied to a 1D VTI model. We demonstrate four cases of introducing additional information. In the first case, vertical velocity is assumed to be known, and the tomography inverts only for Thomsen's δ and ε profiles using surface seismic data alone. In the second case, tomography simultaneously inverts for all three VTI parameters, including vertical velocity, using a joint data set that consists of surface seismic data and vertical check-shot traveltimes. In the third and fourth cases, sparse depth markers and walkaway vertical seismic profiling (VSP) are used, respectively, to supplement the seismic data. For all four examples, tomography reliably recovers the anisotropic velocity field up to a vertical resolution comparable to that of the well data. Even though walkaway VSP has the additional dimension of angle or offset, it offers no further increase in this resolution limit. Anisotropic tomography with well constraints has multiple advantages over other approaches and deserves a place in the portfolio of model-building tools.

INTRODUCTION

Anisotropic depth imaging continues to gain popularity, and vertical transverse isotropy (VTI) has become a default model type for depth imaging in many areas. This progression from isotropy to anisotropy has been driven by increasingly stringent requirements on image positioning errors in true geologic depth. However, estimating the anisotropic model from seismic data alone is known to be a highly nonunique process, even for layered geologic environments (Grechka et al., 2002). Although many different depth models might flatten seismic gathers, only one of them gives the correct depth positioning. A practical solution to this problem is to inject well measurements and all possible a priori information to constrain the anisotropic models. Conceptually, such an approach is universally accepted; however, practical implementations vary substantially.

For 1D media, a simple layer-stripping approach allows estimation of VTI parameters provided either vertical velocity or a set of depth markers is known along the well (Morice et al., 2004). For layered media with homogeneous layers and dipping interfaces, stacking velocity tomography can recover anisotropic parameters provided similar borehole constraints are attached (Wang and Tsvankin, 2009). In a more general case of layered media, model-based inversion of prestack traveltimes allows some estimation of velocity and anisotropy from seismic and well data (Sexton and Williamson, 1998). Iterative tomographic inversion of residual moveout after prestack depth migration (Behera and Tsvankin, 2009) might allow handling of blocky media with horizontal/vertical velocity gradients, provided anisotropy is constant per block and some velocity information is known. Manual trial and error inversion can be used for the most general model type (Bear et al., 2005), but it puts the burden of arriving at an acceptable solution on the interpreter.

Available automated methods suffer from at least two serious restrictions. First, many of them rely on inverting seismic signatures that are hard to estimate such as prestack traveltimes. Second, they are applicable to certain types of models only (1D homogeneous layers, layers with gradients, and others). Manual inversion could be applied to more complex cases, but lack of automation makes the process highly tedious and the final result subjective. As a result,

Manuscript received by the Editor 30 November 2009; revised manuscript received 8 March 2010; published online 5 October 2010.
[1]Formerly WesternGeco/Schlumberger, Houston, Texas, U.S.A.; presently Saudi Aramco, Dhahran, Saudi Arabia. E-mail: a_bakulin@yahoo.com.
[2]WesternGeco/Schlumberger, Houston, Texas, U.S.A. E-mail: woodward2@slb.com; nichols0@slb.com; kosypov@slb.com; ozdraveva@slb.com.

none of the available methods receives widespread approval or use in the oil and gas industry, wherein most velocity model building is performed with highly automated, ray-based, postmigration hybrid grid tomography (Wyatt et al., 1997; Woodward et al., 1998, 2008; Zhou et al., 2003, 2004; Jones et al., 2007). These types of tomography make no assumptions about the model type and can generally handle both "hard" geology (with highly contrasting properties) as well as "soft" geology (compaction-driven velocity regimes). Therefore, from a practical standpoint, it might be useful to adapt existing reflection tomography for anisotropic inversions by supplementing it with the appropriate well data. We pursue this approach in this study.

LOCALIZED REFLECTION TOMOGRAPHY

Reflection tomography uses the redundancy in subsurface images to recover velocity information. One image volume can be derived for each offset or opening angle of the input data. The depth variation of reflection events across offset is defined as residual moveout (RMO). Typically, RMO is analyzed on common-offset image volumes sorted to common-image-point (CIP) gathers (Wyatt et al., 1997; Woodward et al., 1998, 2008; Zhou et al., 2003, 2004). When all data are imaged into the same depth (no residual moveout), the velocity model has optimized the data focusing; when there is nonzero RMO, we can trace rays through the model to determine which parts of the model must be updated to flatten the moveout and improve the focusing. Therefore, standard industry grid tomography generates and solves linearized equations that update the earth model to reduce residual moveout on CIP gathers.

In present practice, tomography updates only the vertical velocity field (V_{P0}); global volumes of Thomsen parameters δ and ε are built without tomography and then frozen. This practice is driven by the well-known fact that multiparameter anisotropic inversion is highly nonunique in the absence of additional constraints such as well data. Therefore, if multiparameter inversion is attempted on VTI grid models using only residual migration equations for flattening RMO data, it almost always results in "patchy" anisotropic models that have geologically implausible V_{P0}, δ, and ε fields.

Although we are not challenging these established practices for deriving global velocity models (on the exploration scale), we believe that there is room for multiparameter tomographic inversion on a more local scale (specifically around wells). For reflection tomography to invert for multiple parameters of the anisotropic velocity field at a specific location (e.g., velocity and Thomsen parameters), we must add two constraints:

1) Jointly invert the surface seismic RMO data with at least one type of well data (e.g., velocity measured in wells, traveltimes from check shots or VSP, or depth-marker mis-ties).
2) Constrain the 3D shapes of the (anisotropic) parameter updates away from the well with a priori information, such as steering them along dip with preconditioning.

The implementation details of the joint inversion and update shaping away from the well are relegated to Appendix A. Here, we mainly focus on the application of this technique to several practical scenarios typical for anisotropic model building.

It is important to note that even with the introduction of these two constraints into tomography, well information remains local by its nature. The definition of "local" will always involve an educated guess about where well data remain valid in a volume to avoid nonuniqueness at the local scale. In the case of a single well or sparsely located wells, it makes sense to invert only for a local anisotropic velocity model around the well, where "local" is tied to the spread length. Where earth properties might be tied to interpretable geology, "local" could extend beyond a spread length.

Incorporating borehole measurements of symmetry-axis velocity

One of the simplest ways to introduce well data is by measuring symmetry-axis velocity in boreholes and assigning this velocity to a local volume around the well. For example, such an approach might work well for a subsurface that is close to a 1D VTI medium and where velocity is measured along a vertical borehole using check-shot or acoustic logs. In this case, one can assume that well velocity remains laterally invariant around the borehole according to the 1D approximation. The classic example of this approach is manual 1D layer stripping (Tsvankin, 2001; Morice et al., 2004), which is popular in the industry.

A modification of this strategy might also be applied to laterally varying media for which the initial model was built from seismic data and then calibrated to wells. One possible practice is to derive the ratio between well and initial seismic velocity along one or several boreholes and then to extrapolate the ratio out into the model volume, thus "scaling" the seismic vertical velocity (in a volume) to match the wells. This method relies on the assumption that, after scaling, velocity becomes close to the true velocity between the wells. Such a case of a borehole-calibrated velocity field (i.e., a velocity field constrained along the symmetry axis) is handled easily by tomography (see Appendix A) because post-scaling flattening of the gathers is achieved by updating only Thomsen parameters ε and δ. This is a well-posed problem for VTI media, provided the data have large offsets. When a borehole is drilled at an angle to the symmetry axis of the anisotropic media, then a more general approach is required as described below.

Kinematic information from check-shot, VSP, or log data

Very often, well data are represented by first-arrival traveltimes picked on borehole seismic data such as check shots or walkaway VSP surveys. For a horizontally layered VTI medium and a vertical well, check-shot measurements can be directly inverted for a profile of velocity along the symmetry axis. However, in the case of a deviated well, laterally varying media, more complex symmetry such as tilted transverse isotropy (TTI), or VSP data acquired with a nonzero offset, a more general method is required. In our approach, we conduct two-point ray tracing in the initial model, compute predicted traveltimes, and then come up with linear equations relating the traveltime errors to changes in the model properties (see Appendix A). These equations are combined with a similar set of equations for RMO from the surface seismic data (Woodward et al., 2008) and are jointly solved to come up with a tomographic update that is consistent with both data types.

Acoustic log data can be handled using a similar methodology by treating log data as an extension of the check-shot survey in which the source moves along the well with the receiver. In practice, one might prefer to integrate (upscale) sonic traveltime to longer segments of the well (for example, equal to one-half the seismic wavelength). After that, these data can be treated exactly the same way as other borehole seismic measurements and modeled by ray tracing with a moving downhole source and downhole receiver. It should be noted that such upscaling might not be necessary because usually the smoothing length in tomography is much longer than the well-data sample interval. Regularization inside the tomography (Appendix A) will automatically smooth high-frequency well data.

Well markers

Another common type of well data consists of so-called well markers. By performing a seismic-to-well tie or by analyzing log data from the well, one can identify the actual location in well depth of the strongest reflections seen on the seismic data. The well depth of the interpreted markers is often in disagreement with the seismic depth of those same events as interpreted on a depth image migrated with the initial velocity model. The difference between the two, often referred to as a well mis-tie, becomes a valuable constraint for updating an anisotropic velocity model. One way to achieve this is to ray trace a marker event in the current velocity model using the current seismic depth and seismic dip. Such ray tracing with zero offset or finite offset simulates the rays that would be reflected at the marker location if we were to have a local plane reflector at this point. A linear equation then can be written to update the anisotropic velocity field along the raypath to relocate the marker from seismic depth to well depth (Appendix A). Such equations strongly constrain tomography problems that otherwise seek only to flatten the residual moveout of seismic events with the floating-reflector approach (Woodward et al., 2008). Therefore, marker-related equations remove or reduce nonuniqueness and allow us to invert simultaneously for velocity and anisotropy parameters.

Egozi et al. (2006) suggest a method to use interpolated mis-tie surfaces (derived from multiple wells) for updating a TTI velocity field; however, their approach appears to solve mis-tie equations without seismic data and to update only velocity along the symmetry axis. Although this might work for horizontal marker events in a VTI medium, for a general case of dipping reflectors in a TTI/VTI medium, vertical positioning is controlled by all three parameters (symmetry-axis velocity V_{P0}, ε, and δ): updating only symmetry-axis velocity to eliminate the mis-tie will lead to a biased estimate of velocities. In our approach, we jointly invert well marker and surface seismic RMO data and simultaneously update all three parameters, thus avoiding a bias toward any single parameter (Appendix A). Such an approach is applicable to VTI and TTI media without any restrictions.

SYNTHETIC EXAMPLE

Let us apply anisotropic tomography with well constraints to a simple deepwater model (Figure 1). The subsurface is represented by a horizontally layered VTI sediment model. The model has smooth vertical variation of velocity and anisotropy (Figure 1a and b). Two pronounced velocity inversions are present in the model. A cable length of 12 km is assumed. A prestack gather computed with anisotropic ray tracing is shown in Figure 1c. Reflected events from 49 interfaces of density contrast are located every 200 m.

It is known that for this type of model geometry, long-spread reflection data will constrain only two parameters: $V_{NMO} = V_{P0}\sqrt{1+2\delta}$ is constrained by short-spread moveout, whereas $\eta \approx \varepsilon - \delta$ can be estimated from long-offset moveout (Tsvankin, 2001). Here, V_{P0}, ε, and δ are the three independent Thomsen parameters that completely describe the VTI velocity field, whereas η is a derivative parameter useful for analysis. If no well information is available, then seismic data can be equivalently imaged with a series of models that preserve $V_{NMO} = V_{P0}\sqrt{1+2\delta}$ and η, but that have different V_{P0}, ε, and δ fields (Tsvankin, 2001; Grechka et al., 2002). To recover the true model, we need to provide additional constraints to the tomography. Here, we examine four possible scenarios of localized tomography with well constraints:

1) Use the correct vertical velocity field and invert surface seismic data for anisotropy parameters ε and δ.
2) Jointly invert surface seismic and vertical check-shot data for three parameters: V_{P0}, ε, and δ.
3) Jointly invert surface seismic data and a set of depth markers for three parameters: V_{P0}, ε, and δ.
4) Jointly invert (for three parameters V_{P0}, ε, and δ) surface seismic data and traveltimes recorded by two levels of walkaway VSP.

In all examples, we use the WesternGeco reflection tomography described by Woodward et al. (2008). We assume an isotropic initial model. In commercial practice we would likely start with the regional nonzero anisotropic profiles that are expected to be closer to the desired true model, thus reducing the number of iterations required. We found that similar solutions are obtained eventually, regardless of the initial model.

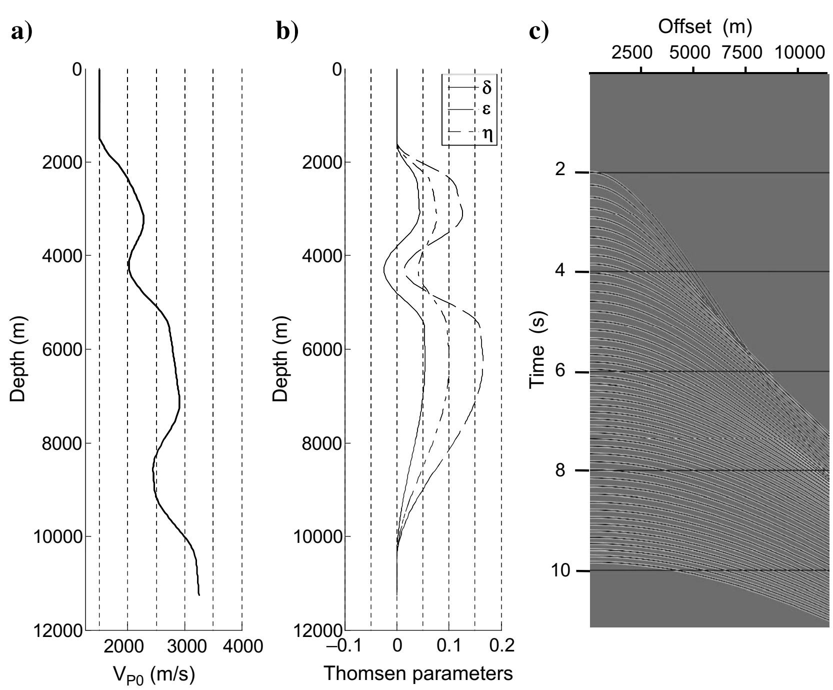

Figure 1. Deepwater 1D VTI model used for tomography: (a) vertical velocity, (b) anisotropic parameters, (c) prestack gather. Water depth is 1500 m.

1. Two-parameter tomographic inversion after fixing vertical velocity from well data

In this scenario, we assume that vertical velocity V_{P0} was estimated from acoustic logs or check-shot data. Thus, tomography is given a true vertical velocity field and is tasked to perform simultaneous inversion for Thomsen's δ and ε using all available offsets. To regularize the grid tomography, we apply smoothness constraints in all three directions (Appendix A). Because our intent is to invert for a laterally invariant model, the horizontal smoothing scales are set equal to the lateral dimensions of the local model and only the vertical scale is varied. To avoid small-scale artifacts and to prevent any potential instabilities, we used a conservative scheme for the vertical smoothness constraints. For the first two iterations, we opted to recover the smoothest part of the vertical anisotropy profile solving down to a vertical scale of 4000 m (Figure 2). The third and fourth iterations were allowed to update the vertical anisotropy profile with variations on the order of 1350 and 750 m, respectively, and they promptly resolved the true profile highs and lows. After the last iteration, the standard deviations of Thomsen's ε and δ from their true values are 0.006 and 0.011, respectively, across the entire well depth of 11 km.

Therefore, we have demonstrated that by using grid tomography with smoothness constraints equivalent to horizontal layering, we have reproduced results typically achieved with layer-based inversions (Tsvankin, 2001) or manual layer stripping (Morice et al., 2004). Sharp interfaces are not recovered by grid tomography unless they are specifically introduced. Nevertheless, grid tomography has several other advantages that outweigh this and other limitations in practical circumstances:

- It does not require defining explicit interfaces for inversion.
- It allows flexible control of spatial resolution without regridding the model (achieved by preconditioning with smoothness constraints as explained in Appendix A).
- It uses all seismic events simultaneously, therefore avoiding error amplification with depth.
- It removes the subjectivity of manual layer-stripping approaches.

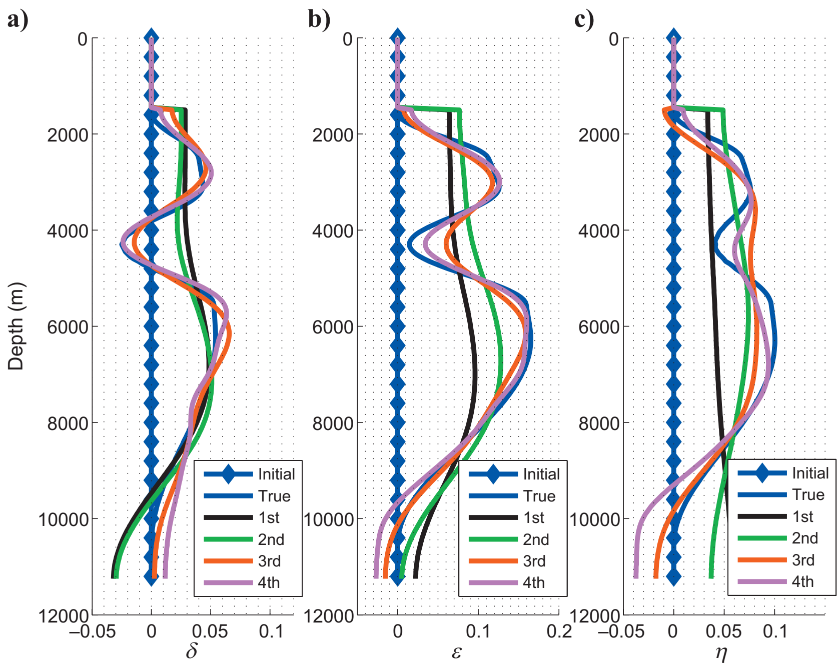

Figure 2. Convergence of two-parameter anisotropic inversion after fixing vertical velocity. Anisotropy profiles after each iteration (a, b, c) are shown with initial and true models.

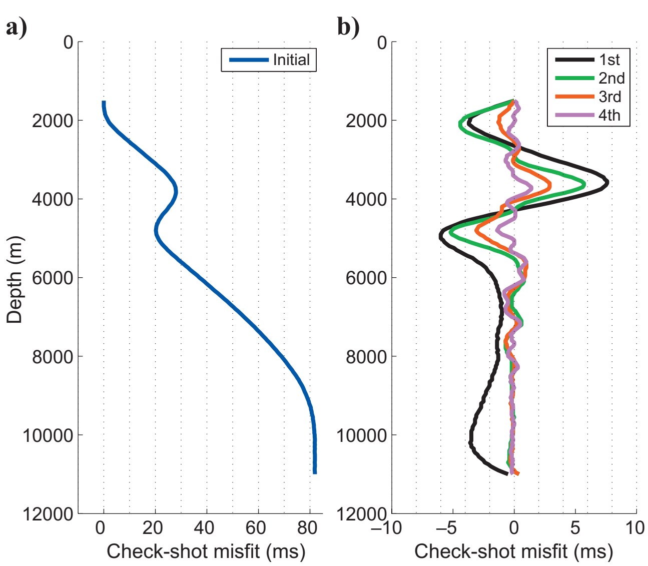

Figure 3. Misfit in check-shot traveltimes for (a) initial model and (b) all subsequent tomographic iterations. Misfit is computed as a difference between measured and predicted traveltimes.

2. Three-parameter inversion of seismic and check-shot data

Although the previous approach can be applied in the case of vertical wells and VTI, introducing check-shot or VSP data, or acoustic logs, requires a more general methodology. We illustrate this in a second scenario, wherein we invert simultaneously for three VTI parameters (V_{P0}, ε, and δ) using joint tomographic inversion of vertical check-shot traveltimes and surface-seismic data. As explained in Appendix A, for each source-receiver pair of the check shot, we perform two-point ray tracing in an initial model, compute traveltimes, and come up with the additional "well data" equations for joint tomographic inversion. Similarly to the previous example, horizontal scales are kept equal to the size of the model, and the vertical smoothing scale is varied from 4000 to 650 m. We emphasize that the same horizontal scales are applied to all three parameters (V_{P0}, ε, and δ). This means that vertical velocity, constrained by check-shot data around the well, is effectively propagated in a 1D fashion away from the well. As a result, grid tomography inverts for a completely layered model.

The check shot consists of 191 observations recorded over depths ranging from 1.5 to 11 km. Because the check-shot misfit has far fewer data points compared to the seismic residual moveout observations, it was weighted to ensure that tomography treats check-shot and seismic data on an equal footing (see Appendix A). In this case, the initial model is again isotropic, but with an incorrect velocity equal to the actual interval NMO velocity. Figure 3a shows that the initial model has too-fast vertical velocity and the check-shot misfit reaches 80 ms at depth. After the first iteration, the maximum misfit reduces to less than 10 ms (Figure 3b). After the fourth and final iteration, we observe zero-mean check-shot errors that are less than 1.5 ms. This result is reasonable given a likely measurement error of 1 ms, and our decision to find the best smooth model that fits the data. After the last iteration (Figure 4), the standard deviation of Thomsen's ε and δ from their true values are 0.008 and 0.013, respectively, across the entire well depth of 11 km, which is slightly less accurate than in the previous example.

Note that the vertical resolution of the well data (i.e., check-shot sampling of 50 m) is much finer than the vertical scale of the features in the velocity models, and therefore accurate profiles are recovered. We shall see that our conclusions are different when the well data have a lower vertical resolution. The use of different initial models leads to quantitatively similar solutions because layered VTI inversion is a well-posed problem that has a unique solution.

3. Three-parameter inversion of seismic data and markers

In a third scenario, we use low-resolution well data consisting of six depth markers that are shown for the initial model in Figure 5a. Tomography inverts for three VTI parameters using a joint data set consisting of seismic data and well-depth mis-ties. As explained in Appendix A, marker-related equations are derived by doing bottom-up ray tracing from each marker location as interpreted on the seismic image. In this example, we used only zero-offset (vertical) rays traced from each seismic marker. As in the VSP case, the contribution of each marker's misfit must be given sufficient weight in the cost function to ensure that tomography simultaneously flattens the image gathers and eliminates the mis-ties. (See Appendix A for details.)

As in the previous example, the initial model is isotropic with an incorrect vertical velocity equal to the actual interval NMO velocity. Figure 5b shows that tomography efficiently reduces the mis-ties by adjusting the vertical velocity while simultaneously flattening the gathers by aggressively updating the anisotropy parameters (Figure 6). After four iterations, tomography accomplishes the goal of making all the image gathers flat while minimizing the mis-ties to less than 7 m. However, only an approximation to the true anisotropic model is recovered due to the velocity-depth ambiguity that exists between the marker points (Figure 6). As a result, mis-ties for events that did not participate in tomography might remain noticeable. For example, mis-ties above the first marker are up to 25 m (Figure 5b). Due to the interplay between all three VTI parameters, errors in velocity result in a less accurate estimation of ε and δ, in particular above the first marker. Such artifacts

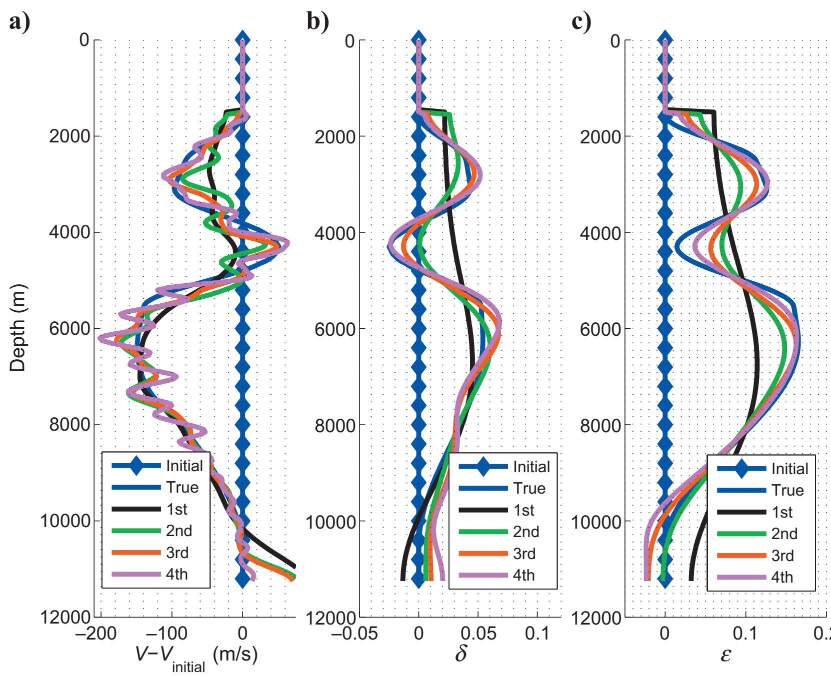

Figure 4. Convergence of three-parameter anisotropic inversion of seismic and check-shot data. (a) Velocity and anisotropy profiles (b, c) after each iteration, with initial and true models. Velocity is shown as the difference between the current velocity at each iteration and the initial velocity profile.

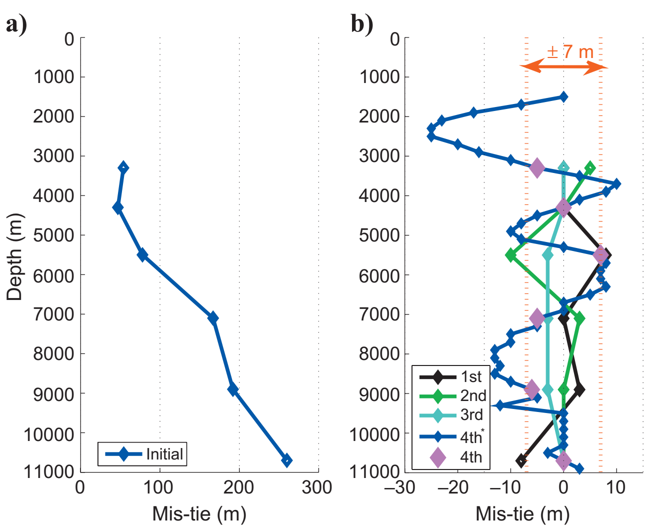

Figure 5. Mis-tie for (a) initial model and (b) all subsequent tomography iterations. After the last iteration, all mis-ties used by tomography are (b) less than 7 m. Note that whereas depth mismatches for events used by tomography are small (magenta diamonds or 4th on [b]), mis-ties for other events can reach up to 25 m (blue diamonds or 4th* on [b]).

were not present in the previous example with a check shot because the vertical resolution of the well data was 50 m across the entire section. In this case, the sparse markers are separated by 1000 to 3000 m.

Because the distance between the markers is comparable to the size of the vertical features in the velocity model, we cannot achieve as good a reconstruction as we did with a check shot. Nevertheless, the recovered estimate is still a reasonable approximation to an actual VTI model from the practical perspective of seismic imaging. To remove geologically implausible jumps in anisotropy parameters at the water bottom, one can either edit the top portion of anisotropic profiles (with an equivalent velocity update) or introduce additional tapering constraints into the tomography.

4. Three-parameter inversion of seismic and sparse walkaway VSP data

In a fourth scenario, well data consist of two levels of walkaway VSP: a shallow level at 4500 m and a deeper level at 9000 m. Walkaway VSP is shot along the same 2D line as the surface seismic data. The maximum source-receiver offset is 12 km. We deliberately leave out the check-shot information here because we want to analyze the information content of the sparse walkaway VSP in the context of anisotropic model building. In other words, we attempt to understand whether the additional angle/offset dimension present in walkaway VSP data might in some way compensate for the limited vertical coverage typical of borehole seismic data. The same initial model is used as in the previous two examples. Figure 7a shows VSP traveltime residuals for the initial model ranging from 80 to −120 ms. At zero offset, they agree with Figure 3a and suggest that vertical velocity in the initial model is too fast. However, at large offsets, the residuals have opposite signs suggesting that the Thomsen parameters in the initial model are too small. Three iterations of joint tomographic inversion result in a model that has VSP residuals of less than 4 ms at all offsets (Figure 7b) and flat CIP gathers.

It is important to stress that all iterations have been performed with a vertical scale of 4000 m applied to all parameters, and, therefore, only an approximate low-frequency version of the anisotropic velocity model is recovered (Figure 8). Note that this scale is in approximate agreement with the vertical resolution of the well data (~4500 m). Any attempt to bring the vertical scale down further, to even 2000 m, results in an equivalent VTI model that still satisfies all the data, but diverges from both the true model and its low-frequency trend. Therefore we conclude that despite all the additional sampling in the angle domain present in the VSP data from shallow and deep levels, we are unable to uniquely recover vertical details of the layered VTI model that are finer than the distance between shallow and deep levels. We expect that a similar conclusion applies to all VSP acquisition restricted to a relatively small portion of the well. Therefore, to resolve finer vertical details, we would still need dense vertical check-shot or log information.

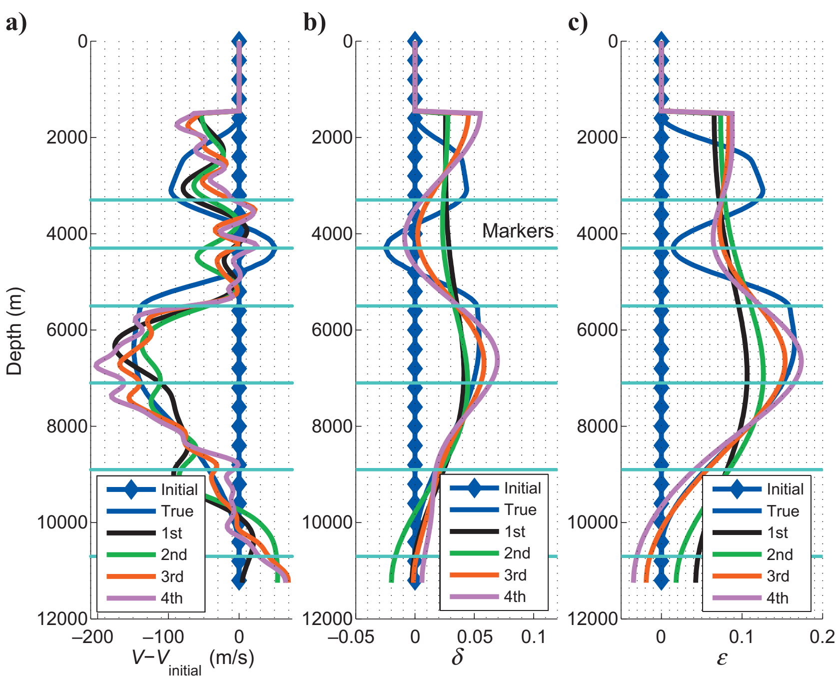

Figure 6. Convergence of a three-parameter anisotropic inversion of seismic and marker data. (a) Velocity and (b, c) anisotropy profiles after each iteration, with initial and true models. Velocity is shown as the difference between current velocity at each iteration and the initial velocity profile.

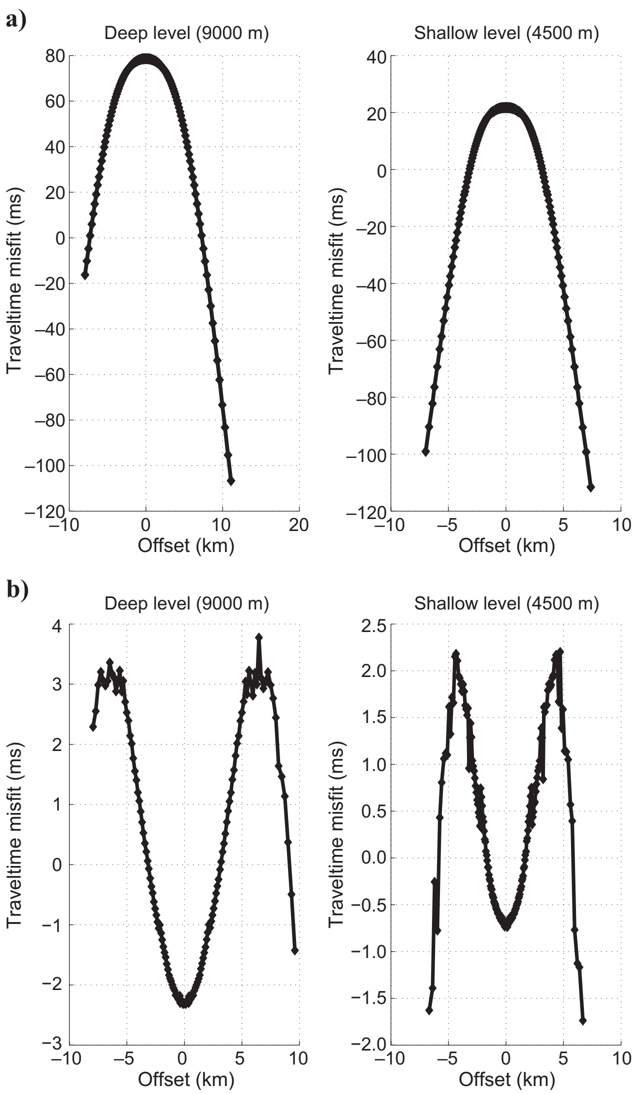

Figure 7. Residuals between measured and computed walkaway VSP traveltimes (a) before and (b) after tomography.

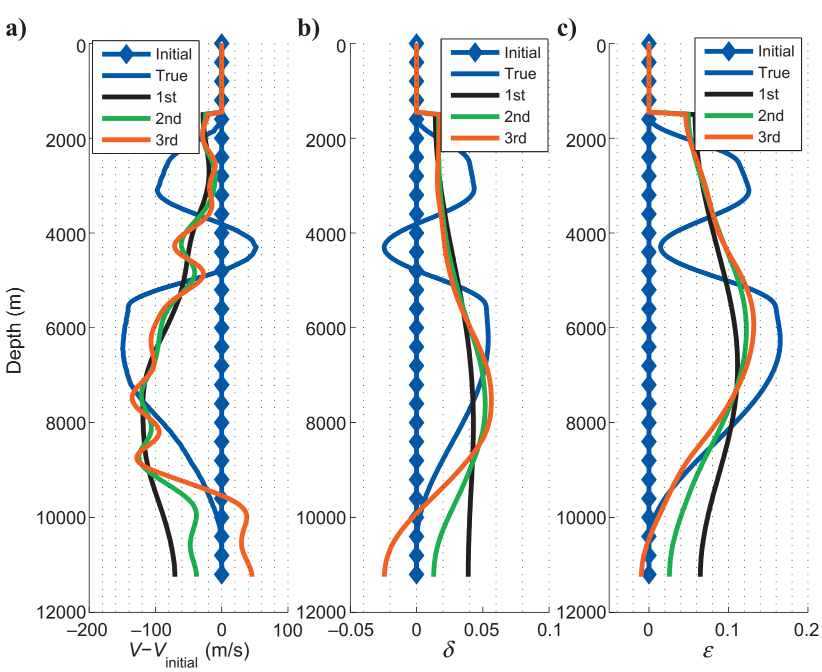

Figure 8. Convergence of a three-parameter tomographic inversion of seismic and walkaway VSP data. (a) Velocity and (b, c) anisotropy profiles, for all iterations of tomography. Note that velocity is shown as a difference between current velocity and initial velocity in a starting model. We used a vertical scale of 4000 m for smoothing all parameters in the tomography, which is comparable to the distance between two levels (4500 m).

CONCLUSIONS

We have outlined a concept and implementation of anisotropic tomography with well constraints. We have demonstrated that, by localizing the tomography to the volume near the well and by introducing and extrapolating proper constraints from the well, we can eliminate or reduce nonuniqueness and recover a good estimate of Thomsen parameters and velocity around the well for layered VTI models. We presented four practical scenarios wherein well data are introduced by either fixing vertical velocity, providing vertical check-shot traveltimes, introducing depth markers, or measuring walkaway VSP traveltimes.

In all cases, a good approximation to the actual VTI velocity field is recovered by joint tomographic inversion. The accuracy of the recovered field is controlled by the vertical resolution of the available well data: the best reconstruction is achieved with correct and fixed vertical velocity. Slightly less accurate is reconstruction with dense vertical check-shot traveltimes. Sparse depth markers allow recovery of an approximate model that still has some highs and lows in correct places; however, it becomes inaccurate between the markers. The worst reconstruction is achieved with two widely spaced levels of walkaway VSP wherein only the low-frequency trend (without highs and lows) is recovered. Thus, achievable vertical resolution in anisotropy profiles is related to vertical resolution of the well data. The choice of the initial model plays a minor role: starting from a different initial model leads to practically the same solution with slight variations. We emphasize that these ambiguities have been observed for strictly layered VTI models when data are noise free and ideal (i.e., large offsets and dense events picked for tomography). Therefore, in practice with less ideal data and lateral heterogeneity, we expect less certain results.

Localized tomography could replace the presently used anisotropic calibration approach that uses manual layer-stripping 1D inversion, or it can be used as a good starting guess for a manual refinement. We anticipate that this approach of borehole-constrained tomography can be applied to inversion for anisotropy in 2D and 3D models, provided that smoothing constraints following the geology are used. The tomographic setup described is deliberately done in a general framework so that no modifications are required to treat the cases of anisotropic calibration with deviated wells and more complex anisotropic models such as tilted transverse isotropy. These examples will be the subject of future studies.

ACKNOWLEDGMENTS

We thank Dmitry Alexandrov (summer intern from St. Petersburg State University) for help with generating the synthetic data set.

APPENDIX A

REFLECTION TOMOGRAPHY AND ITS MODIFICATION TO JOINT INVERSION

The present industry standard for velocity model building in the depth domain is to analyze residual moveout across offset on CIP gathers (Stork, 1992; Wyatt et al., 1997; Woodward et al., 1998, 2008; Zhou et al., 2004; Osypov et al., 2008). Rays are traced through a background model to create equations that relate changes in earth properties to changes in moveout across offset. For the work in this study, we used linearized residual migration equations based on the formulation of Stork (1992):

$$\begin{aligned} z_h' &= z_h + \Delta z \\ &= z_h - \sum_i (\partial t/\partial \alpha_i * \Delta \alpha_i) * V/(2*\cos\theta*\cos\phi). \end{aligned} \quad \text{(A-1)}$$

The prime indicates a residually migrated reflector depth; z_h is depth as a function of offset (or angle) h, i indicates a node on the property grid, θ is the angle of incidence for the reflection, ϕ is the reflector dip, V is the effective velocity at the reflector, and $\partial t/\partial \alpha_i$ is the change in traveltime corresponding to a change in property α at node i. Properties α might be velocity or slowness and/or Thomsen parameters ε and δ.

The goal of surface seismic tomography is to find property perturbations that will minimize the residual moveout of depth picks that were residually migrated with a model updated with the perturbations, i.e., that will minimize $z_h' - z_0'$, where z_h' is a residually migrated nonnear-offset pick and z_0' is a residually migrated near-offset pick. The basic tomography update equation is formed by subtracting pairs of equation A-1's corresponding to nonnear-offset and near-offset picks and accumulating the picked depth errors on the right side of equation

$$\mathbf{L}\Delta\alpha = \Delta z, \quad \text{(A-2)}$$

where $\mathbf{L}$ contains the geometry and background model terms of equation A-1; the expression Δz represents picked moveout errors relative to near offset.

Because surface seismic problems are underdetermined, we regularize the problem by rewriting the equation as

$$\mathbf{PLSW}\Delta\alpha' = \mathbf{P}\Delta z. \quad \text{(A-3)}$$

Our update is $\Delta\alpha = \mathbf{SW}\Delta\alpha'$; $\mathbf{P}$ is a row-weighting (diagonal) matrix (Van der Sluis and van der Vorst, 1987); $\mathbf{SW}$ is a preconditioner that constrains the shape of our update, following the model reparameterization work of Harlan (1995) and Fomel (1997). In the language of Tarantola (2005), it is the factored square root of a model covariance assumed as an a priori constraint. For the 1D problem in this study, $\mathbf{S}$ is an isotropic smoother applied as a 3D convolution, with user-specified scale lengths in x, y, and z. For 2D or 3D problems, it might be an inverse steering filter used to smooth along a geologic dip (Clapp et al., 1998). The expression $\mathbf{W}$ is a diagonal column-weighting matrix that normalizes the model parameters for variations in illumination and for the simultaneous solution of properties with different magnitude ranges.

We solve equation A-3 using the LSQR algorithm (Paige and Saunders, 1982), minimizing the objective function

$$\Phi = \|\mathbf{PLSW}\Delta\alpha' - \mathbf{P}\Delta z\|^m + \lambda^2\|\Delta\alpha'\|^n. \quad \text{(A-4)}$$

Selection of m and n determines the norms used to quantify the data misfit and the model perturbations, respectively. The first term represents a weighted measure of the residual moveout from all seismic gathers, whereas the second term introduces regularization that penalizes large departures from the initial model (Van der Sluis and Van der Vorst, 1987).

When we add borehole data into tomography, we add rows to the linear equation matrix of equation A-2. For well mis-tie data, we add an equation in depth to minimize $z_h' - z_{\text{well}}$ with equation A-1. For check-shot or VSP data, our data errors are traveltime errors instead of depth errors. Instead of tracing rays to form residual migration equations, we use a two-point ray tracer to form equations relating changes in earth properties to changes in traveltime,

$$\Delta t = \sum_i (\partial t / \partial \alpha_i * \Delta \alpha_i). \quad (A\text{-}5)$$

Because we never run linearized tomography problems to complete convergence (that would be very slow and the result likely invalid), we use row weighting to normalize the importance of the well-constraint equations relative to the residual moveout equations in the objective function equation A-4. Our rule of thumb is to put terms in the diagonal row-weighting matrix **P** to make the impact of the well-data errors equal to the impact of the RMO errors for the localized tomography problem. We also use row weighting to normalize the combination of time and depth errors.

REFERENCES

Bear, L. K., T. A. Dickens, J. R. Krebs, J. Liu, and P. Traynin, 2005, Integrated velocity model estimation for improved positioning with anisotropic PSDM: The Leading Edge, **24**, 622–634.

Behera, L., and I. Tsvankin, 2009, Migration velocity analysis for tilted transversely isotropic media: Geophysical Prospecting, **57**, 13–26.

Clapp, R. G., B. L. Biondo, S. B. Fomel, and J. F. Claerbout, 1998, Regularizing velocity estimation using geologic dip information: 68th Annual International Meeting, SEG, Expanded Abstracts, 1851–1854.

Egozi, U., M. Yates, J. Omana, B. Ver West, N. Burke, M. Mesa, E. Moreno, J. Checa, M. Martinez, H. Alfonso, and J. E. Calderon, 2006, A comprehensive velocity model building approach — Cusiana Cupiagua Sur TTI PSDM: 76th Annual International Meeting, SEG, Expanded Abstracts, 525–529.

Fomel, S., 1997, On model-space and data-space regularization: A tutorial: Stanford Exploration Project Report 94, 141–160 accessed 13 July 2010; http://sepwww.stanford.edu/data/media/public/docs/sep94/toc_html/.

Grechka, V., I. Tsvankin, A. Bakulin, J. O. Hansen, and C. Signer, 2002, Joint inversion of PP and PS reflection data for VTI media: A North Sea case study: Geophysics, **67**, 1382–1395.

Harlan, W. S., 1995, Regularization by model reparameterization, http://billharlan.com/pub/papers/regularization.html, accessed 10 January 2008.

Jones, I. F., M. J. Sugrue, and P. B. Hardy, 2007, Hybrid gridded tomography: First Break, **25**, 35–41.

Morice, S., J.-C. Puech, and S. Leaney, 2004, Well-driven seismic: 3D data processing solutions from wireline logs and borehole seismic data: First Break, **22**, 61–66.

Osypov, K., D. Nichols, M. Woodward, O. Zdraveva, and C. E. Yarman, 2008, Uncertainty and resolution analysis for anisotropic tomography using iterative eigendecomposition: 78th Annual International Meeting, SEG, Expanded Abstracts, 3244–3249.

Paige, C. C., and M. A. Saunders, 1982, LSQR: An algorithm for sparse linear equations and sparse least squares: Association for Computing Machinery Transactions on Mathematical Software, **8**, 43–71.

Sexton, P., and P. Williamson, 1998, 3D anisotropic velocity estimation by model-based inversion of pre-stack traveltimes: 68th Annual International Meeting, SEG, Expanded Abstracts, 1855–1858.

Stork, C., 1992, Reflection tomography in the postmigrated domain: Geophysics, **57**, 680–692.

Tarantola, A., 2005, Inverse problem theory and methods for model parameter estimation: Society for Industrial and Applied Mathematics.

Tsvankin, I., 2001, Seismic signatures and analysis of reflection data in anisotropic media: Elsevier Science.

Van der Sluis, A., and H. A. van der Vorst, 1987, Numerical solution of large, sparse linear algebraic systems arising from tomographic problems, *in* G. Nolet, ed., Seismic tomography with applications to global seismology and exploration geophysics: Reidel Publishing, 49–84.

Wang, X., and I. Tsvankin, 2009, Stacking-velocity tomography with borehole constraints for tilted TI media: 79th Annual International Meeting, SEG, Expanded Abstracts, 2352–2356.

Woodward, M., P. Farmer, D. Nichols, and S. Charles, 1998, Automated 3D tomographic velocity analysis of residual moveout in prestack depth migrated common image point gathers: 68th Annual International Meeting, SEG, Expanded Abstracts, 1218–1221.

Woodward, M., D. Nichols, O. Zdraveva, P. Whitfield, and T. Johns, 2008, A decade of tomography: Geophysics, **73**, no. 5, VE-5–VE11.

Wyatt, K. D., P. Valasek, S. B. Wyatt, and R. M. Heaton, 1997, Velocity and illumination studies from horizon-based PSDM: 67th Annual International Meeting, SEG, Expanded Abstracts, 1801–1804.

Zhou, H., S. H. Gray, J. Young, D. Pham, and Y. Zhang, 2003, Tomographic residual curvature analysis: The process and its components: 73rd Annual International Meeting, SEG, Expanded Abstracts, 666–669.

Zhou, H., D. Pham, S. Gray, and B. Wang, 2004, Tomographic velocity analysis in strongly anisotropic TTI media: 74th Annual International Meeting, SEG, Expanded Abstracts, 2347–2350.